Published in final edited form as:
J Inorg Organomet Polym Mater. 2013 January 1; 23(1): 227–232. doi:10.1007/s10904-012-9772-y.

Patterning of Protein/Quantum Dot Hybrid Bionanostructures

Vikas Nandwana[a], **Rubul Mout**[a], **Yi-Cheun Yeh**[a], **Stefan Dickert**[b], **Mark T. Tuominen**[b], and **Vincent M. Rotello**[*,a]

[a]Department of Chemistry, University of Massachusetts Amherst, 710 North Pleasant Street, Amherst, MA 01003, USA

[b]Department of Physics, University of Massachusetts Amherst, Amherst, MA 01003, USA

Abstract

Here we demonstrate patterning of protein/quantum dot hybrid bionanostructures *via* electrostatic assembly of engineered negatively charged fluorescent protein with positively charged CdSe/ZnS QD patterns formed through e-beam lithography and post-patterning modification with cationic ligands.

Keywords

Hybrid bionanostructures; patterning; e-beam lithography; electrostatic assembly; bionanofabrication

1 Introduction

Hybrid bionanostructures made of nanoparticles (NPs) and biomolecules are of particular interest in a variety of biomedical applications [1]. Owing to its finite size, a single NP can be conjugated to multiple biomolecules. The conjugation of NPs with biomolecules can be achieved by covalent [2] and non-covalent interactions [3]. While, covalent binding is the most direct approach to create integrated biomolecule–NP conjugates, non-covalent assembly through hydrogen bonding [4], electrostatic [5], metal-coordination [6], and hydrophobic interactions [7] provides a highly modular approach to the biofunctionalization of NPs.

Patterning of hybrid bionanostructures can be used to generate multifunctional ordered architectures for protein arrays [8], biosensors [9], and tissue engineering [10]. Such artificial biochips can be fabricated by selectively immobilizing biomolecules on pre-patterned surfaces of NPs *via* a variety of coupling chemistries [11]. The nanopatterned surface provides a higher density of reaction sites for biomolecules [12]. The surface properties of the patterns can be tailored by choosing NPs with appropriate functionality while the unique optical [13], electronic [14], mechanical [15], and magnetic properties [16] of the NPs can be utilized to serve a particular function. For example, gold NPs were assembled to provide a pathway for measurement of electrical signal in biosensor microdevices [17], while magnetic NPs were used to guide the assembly of multifunctional superstructures on a ferromagnetic surface [18].

[*]Phone: +1 413-5452058, Fax: +1 413-5454490, rotello@chem.umass.edu.

Supplementary Material
Synthesis of TOPO-QDs, synthesis of cationic ligand, preparation of cationic QDs, XPS of cationic QD film before and after e-beam exposure, fluorescence images and intensity map of TOPO-QD pattern before and after incubation in tdTomato solution.

Here we demonstrate patterning of protein/quantum dot (QD) bionanostructures *via* integration of "top-down" and "bottom-up" approaches. First, patterns of positively charged CdSe/ZnS QDs were fabricated *via* e-beam lithography (EBL) [19]. The cationic QD patterns were incubated with a solution of negatively charged fluorescent protein. The negative charge allowed the proteins to self-assemble onto the positively charged QD patterns through electrostatic interactions (Scheme 1). Patterns of trioctylphosphine oxide functionalized QDs (TOPO-QDs) [20] that cannot participate in electrostatic interaction were prepared as a control. Using this approach, we fabricated arbitrarily patterned hybrid protein/QD structures with sub-50 nm resolution.

2 Experimental

2.1 Synthesis and functionalization of CdSe/ZnS QDs

TOPO-QDs were synthesized according to previous reports [21] and post-functionalized with cationic ligands *via* a ligand exchange reaction (Section 1-3, ESI). The presence of cationic ligands on the QDs was confirmed by mass spectrometry (Fig. S1, ESI).

2.2 Cloning and expression of tdTomato (tdT)

Genetic engineering manipulation and protein expression were done according to standard protocols. To construct pQE80-6xHis-tdTomato plasmid, tdTomato gene was sub-cloned from pASTA3 plasmid (from Addgene) into BamHI and Hind III (downstream of 6xHis tag) restriction sites of pQE80 expression vector. To produce recombinant proteins, pQE80-6xHis-tdTomato plasmid was transformed into Escherichia coli BL21(DE3) strain. A transformed colony was picked up to grow small cultures in 50 mL 2×YT media at 37°C overnight. The following day, 15 mL of grown culture was inoculated into one liter 2×YT media and allowed to grow at 37°C until the OD reached 0.6. At this point, the protein expression was induced by adding isopropyl-b-D-thiogalactopyranoside (IPTG; 1 mM final concentration) at 25°C. After four hours of induction, the cells were harvested and the pellets were lysed using a microfluidizer. His-tagged fluorescent proteins were purified from the lysed supernatant using HisPur cobalt columns. The integrity and the expression of native protein were determined by 12% SDS-PAGE gel and absorbance spectra. The exact stability of the protein in dry state was not known. However, when the protein was lyophilized, its color was intact which indicates the integrity of tdTomato even in dry states.

2.3 Patterning of cationic QDs

A silicon substrate coated with 100 nm Au was sonicated in isopropyl alcohol (IPA) for 30 minutes and dried in vacuum for 1 hour to remove residual IPA. A solution of cationic QDs (10 mg/mL in methanol) was then filtered and spin-coated at 1000 rpm for 180 seconds onto the substrate, yielding a thin film of 55 nm thickness as measured by profilometer. E-beam writing in the QD films was achieved in a JEOL JSM-7001F thermal field emission SEM with a 30 kV electron acceleration voltage, equipped with a beam blanker and a CAD software lithography module developed by J. C. Nabity Lithography Systems. The working distance was set to 6 mm and the electron dosage for the test pattern was varied between 100 and 10,000 $\mu C/cm^2$. To remove the unexposed QDs, the QD pattern was then developed by washing the substrate with methanol, followed by sonication for 5 minutes and drying in vacuum for 1 hour.

2.4 Protein immobilization

To immobilize the protein on the QD patterns, a solution of tdTomato (5 mM phosphate buffer, pH 7.4) was prepared. The patterned surface was incubated in the solution for 30 minutes. The unbound protein on the surface was removed by rinsing with 5 mM phosphate

buffer. The surface was then immediately imaged by fluorescence and atomic force microscopy (AFM).

2.5 Characterization

Bright field and fluorescence images were obtained using an Olympus IX51 microscope. Fluorescence images were taken under blue (470±20 nm) and green (535±20 nm) light. AFM imaging of the surfaces was done on a Dimensions 3100 (Veeco) in tapping mode using an RTESP tip (Veeco). X-ray photoelectron spectroscopy (XPS) analysis was performed on a Physical Electronics Quantum 2000 spectrometer using a monochromatic Al Kα excitation at a spot size of 10 mm with pass energy of 46.95 eV at 158 take-off angle to probe the topmost layer.

3 Results and Discussion

Recently we have shown resist-free patterning of TOPO-QDs *via* EBL [20] where the e-beam induces crosslinking of the ligands by a radical mechanism [22]. Due to the crosslinking, the QDs anchored on the exposed areas resulting in the patterned nanostructures. These structures, however, were not functionalized for bioconjugation. Here, we extended this approach to pattern cationic QD nanostructures that were used as a template to immobilize a negatively charged protein. A solution of the QDs functionalized with a positively charged ligand was spin coated to prepare cationic QD films. The film thickness of 55 nm was kept constant throughout all the experiments. As a preliminary step for EBL processing, a range of e-beam dosage exposures were explored to find the optimum dosage required to generate stable QDs features with efficient crosslinking. The test pattern was written in the QD films in the form of 5×5 μm^2 boxes while the dosages were varied from 100 $\mu C/cm^2$ to 10,000 $\mu C/cm^2$.

Fig. 1(a) and 1(b) show bright field and fluorescence images of the developed test pattern, respectively. Lack of fluorescence from the background in Fig. 1(b) shows the complete removal of the unexposed QDs from the substrate. The fluorescence intensity map of the test pattern shows a successive drop in the fluorescence intensity with increasing dosages (Fig. 1(c)), associated with the excessive degradation and overexposure of QDs. At initial dosages, while the fluorescence intensity remains stable, the features were not uniform due to insufficient crosslinking. Taken together, Fig. 1(a-c) indicate that stable features with minimal degradation were generated at the optimized dosage of 1400 $\mu C/cm^2$ that was used for subsequent e-beam writing experiments. A UMass logo pattern using the selected dosage (Fig. 1(d)) demonstrates the ability to fabricate arbitrary structures with high specificity using this approach. XPS elemental analysis on the cationic QD films before and after e-beam exposure showed no significant difference, indicating the stability of the cationic functionality to e-beam exposure (Fig. S2, ESI).

A red fluorescent protein tdTomato was engineered to express an overall negative charge to immobilize onto the cationic QD patterns. The choice of tdTomato was based on the spectral overlap of its absorption with CdSe/ZnSe QDs' emission (Fig. 2(a)). To ensure interaction between cationic QDs and anionic tdTomato, a fluorescence titration was performed in solution. The concentration of QDs was kept constant while the concentration of tdTomato was increased. Fig. 2(b) shows steady-state fluorescence spectra of QDs in the presence of tdTomato. The progressive quenching of the QDs emission and a systematic enhancement of the tdTomato emission was observed as concentration of tdTomato was increased from 10 nM to 4μM, suggesting fluorescence resonance energy transfer (FRET) from QDs to tdTomato. The change in the QDs' emission in the presence of tdTomato confirmed interaction between QDs and tdTomato, presumably electrostatic due to their complementary charges.

With QD-tdTomato interaction verified, we next examined the immobilization of tdTomato on the cationic QD patterns by incubating the patterned substrate in a solution of tdTomato. Fig. 3 shows fluorescence images of the QD pattern before and after incubation. Due to emission at 535 nm, the QD pattern showed strong green and very weak red fluorescence before incubation. After incubation, an almost 2-fold decrease in green fluorescence along with a 4 fold increase in red fluorescence confirmed the protein immobilization onto the QD pattern (Fig. 3). As observed in the titration, the green fluorescence of the QD pattern was decreased due to FRET from QDs to tdTomato. In addition, the lack of red fluorescence from the background after incubation showed undesirable non-specific proteins adsorption outside the pattern was minimal. The immobilization of tdTomato onto the QD patterns resulted in an increase in the feature height of 5 nm (Figure S3, ESI), consistent with the deposition of a monolayer of the protein. To determine the specificity of the electrostatic assembly process, an uncharged TOPO-QD pattern was used as a control. In contrast to the cationic QD pattern, no change in the fluorescence of the TOPO-QD pattern was observed after incubation in tdTomato solution (Fig. S4, ESI), confirming the lack of deposition of the protein onto the TOPO-QD pattern. Taken together, these results demonstrate that the protein immobilization was the result of the designed electrostatic interaction between cationic QDs and anionic proteins rather than random protein adsorption.

EBL can produce nanoscale arbitrary structures; hence we next explored patterning of smaller protein/QD structures. The size of the features was tuned from 10 μm to 50 nm while the shape was readily controlled from simple (ring, star, squares) to complex (rose) structures (Fig. 4(a)). Due to the resolution limit of optical microscopy, structural characterization of nanoscale features was done using AFM. We could fabricate as small as 50 nm features (Fig. 4(c)) *via* e-beam induced crosslinking. Fabrication of features smaller than 50 nm required higher e-beam dosages, which led to the degradation of the QDs. The ability to fabricate complex arbitrary nanostructures was shown with the rose pattern where one can clearly see the thorns of the rose (Fig. 4(b)). High magnification AFM images of the patterned protein/QD nanostructures demonstrate the precision and versatility of this approach.

4 Conclusions

We report a versatile approach to fabricate hybrid protein/QD nanostructures *via* integration of “top-down” EBL patterning and “bottom-up” electrostatic assembly. Patterns of cationic QD structures were fabricated *via* EBL and incubated to complementary charged protein, resulting in protein/QD bionanomaterials. With the possibility to pattern nanostructures with multiple functionalities, this approach can be directly applied for immobilizing various combinations of biomolecules. Furthermore, the choice of NPs lends an addition element of control for creating three dimensional multifunctional structures containing multiplexed biomolecules for advanced biomedical applications.

Supplementary Material

Refer to Web version on PubMed Central for supplementary material.

Acknowledgments

V.M.R. acknowledges the NSF (CHE-1025889), MRSEC facilities, and the Center for Hierarchical Manufacturing (DMI-0531171). R.M. was funded by NIH grant GM077173. V.N. was supported as part of the Polymer-Based Materials for Harvesting Solar Energy, an Energy Frontier Research Center funded by the U.S. Department of Energy, Office of Science, Office of Basic Energy Sciences under Award Number DE-SC0001087.

References

1. (a) Medintz IL, Uyeda HT, Goldman ER, Mattoussi H. Nat. Mater. 2005; 4:435. [PubMed: 15928695] (b) De M, Ghosh PS, Rotello VM. Adv. Mater. 2008; 20:4225.(c) Willner I, Willner B. Nano Lett. 2010; 10:3805. [PubMed: 20843088] (d) Saha K, Agasti SS, Kim C, Li X, Rotello VM. Chem. Rev. 2012; 112:2739. [PubMed: 22295941]
2. (a) Niemeyer CM. Angew. Chem. Int. Ed. 2001; 40:4128.(b) Katz E, Willner I. Angew. Chem. Int. Ed. 2004; 43:6042.(c) Pellegrino T, Kudera S, Liedl T, Javier AM, Manna L, Parak WJ. Small. 2005; 1:48. [PubMed: 17193348] (d) Rosi NL, Mirkin CA. Chem. Rev. 2005; 105:1547. [PubMed: 15826019]
3. Verma A, Rotello VM. Chem. Commun. 2005; 303
4. (a) Boal AK, Ilhan F, DeRouchey JE, Thurn-Albrecht T, Russell TP, Rotello VM. Nature. 2000; 404:746. [PubMed: 10783884] (b) Ilhan F, Galow TH, Gray M, Clavier G, Rotello VM. J. Am. Chem. Soc. 2000; 122:5895.(c) Norsten TB, Jeoung E, Thibault RJ, Rotello VM. Langmuir. 2003; 19:7089.
5. (a) Frankamp BL, Boal AK, Rotello VM. J. Am. Chem. Soc. 2002; 124:15146. [PubMed: 12487569] (b) Srivastava S, Verma A, Frankamp BL, Rotello VM. Adv. Mater. 2005; 17:617.
6. Norsten TB, Frankamp BL, Rotello VM. Nano Lett. 2002; 2:1345.
7. Shenhar R, Jeoung E, Srivastava S, Norsten TB, Rotello VM. Adv. Mater. 2005; 17:2206.
8. (a) Zhu H, Snyder M. Curr. Opin. Chem. Biol. 2001; 5:40. [PubMed: 11166646] (b) Fang Y, Frutos AG, Lahiri J. J. Am. Chem. Soc. 2002; 124:2394. [PubMed: 11890761] (c) Inerowicz HD, Howell S, Regnier FE, Reifenberger R. Langmuir. 2002; 18:5263.(d) Lynch M, Mosher C, Huff J, Nettikadan S, Johnson J, Henderson E. Proteomics. 2004; 4:1695. [PubMed: 15174138]
9. (a) Veiseh M, Zareie MH, Zhang MQ. Langmuir. 2002; 18:6671.(b) Haes AJ, Van Duyne RP. J. Am. Chem. Soc. 2002; 124:10596. [PubMed: 12197762]
10. Thissen H, Johnson G, Hartley PG, Kingshott P, Griesser HJ. Biomaterials. 2006; 27:35. [PubMed: 15996730]
11. (a) Mattoussi H, Mauro JM, Goldman ER, Anderson GP, Sundar VC, Mikulec FV, Bawendi MG. J. Am. Chem. Soc. 2000; 122:12142.(b) Wang C, Zhang Y. Adv. Mater. 2005; 17:150.(c) Xu H, Hong R, Lu T, Uzun O, Rotello VM. J. Am. Chem. Soc. 2006; 128:3162. [PubMed: 16522094] (d) Subramani C, Bajaj A, Miranda OR, Rotello VM. Adv. Mater. 2010; 22:5420. [PubMed: 20925103] (e) Schlapak R, Danzberger J, Haselgrü bler T, Hinterdorfer P, Schäffler F, Howorka S. Nano Lett. 2012; 12:1983. [PubMed: 22376238]
12. Taylor ZR, Patel K, Spain TG, Keay JC, Jernigen JD, Sanchez ES, Grady BP, Johnson MB, Schmidtke DW. Langmuir. 2009; 25:10932. [PubMed: 19670836]
13. Kelly KL, Coronado E, Zhao LL, Schatz GC. J. Phys. Chem. B. 2003; 107:668.
14. Kamat PV. J. Phys. Chem. B. 2002; 106:7729.
15. Dai H. Acc. Chem. Res. 2002; 35:1035. [PubMed: 12484791]
16. Lu AH, Salabas EL, Schuth F. Angew. Chem. Int. Ed. 2007; 46:1222.
17. Park S-J, Taton TA, Mirkin CA. Science. 2002; 295:1503. [PubMed: 11859188]
18. Nikitin MP, Zdobnova TA, Lukash SV, Stremovskiy OA, Deyev SM. Proc. Natl. Acad. Sci. U. S. A. 2010; 107:5827. [PubMed: 20231484]
19. Yeh Y-C, Patra D, Yan B, Saha K, Miranda OR, Kim CK, Rotello VM. Chem. Commun. 2011; 47:3069.
20. Nandwana V, Subramani C, Yeh Y-C, Yang B, Dickert S, Barnes MD, Tuominen MT, Rotello VM. J. Mater. Chem. 2011; 21:16859.
21. (a) Peng ZA, Peng XG. J. Am. Chem. Soc. 2001; 123:183. [PubMed: 11273619] (b) Dabbousi BO, Rodriguez-Viejo J, Mikulec FV, Heine JR, Mattoussi H, Ober R, Jensen KF, Bawendi MG. J. Phys. Chem. B. 1997; 101:9463.
22. Seshadri K, Froyd K, Parikh AN, Allara DL. J. Phys. Chem. 1996; 100:15900.

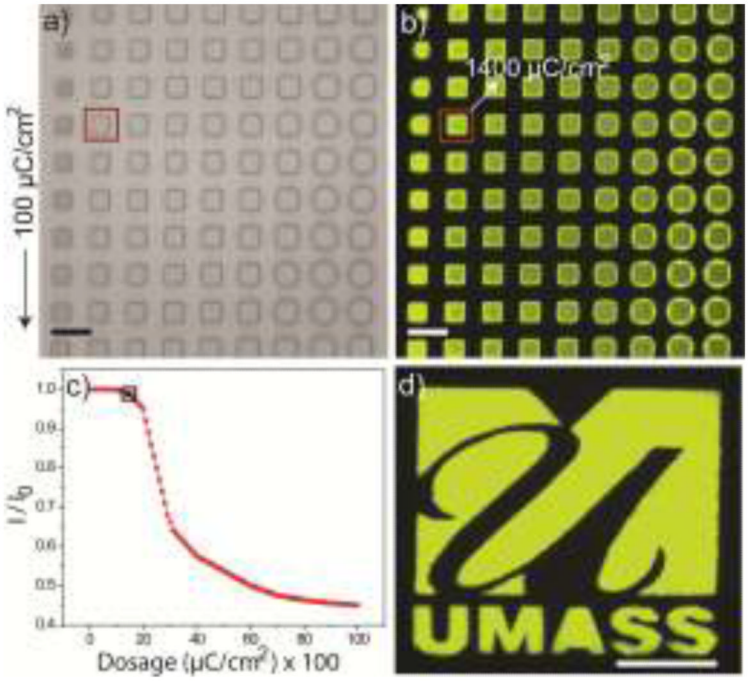

Fig. 1.

(a) Bright field and (b) fluorescence images of QD test pattern with dosages of 100 μC/cm^2 to 10,000 μC/cm^2. (c) Fluorescence intensity (I/I_0) map of the QD structures at increasing e-beam dosages where I_0 is the maximum fluorescence intensity. (d) Fluorescence image of the UMass logo, patterned at 1400 μC/cm^2. Scale bars in 1(a,b) and 1(d) are 10 μm and 5 μm, respectively.

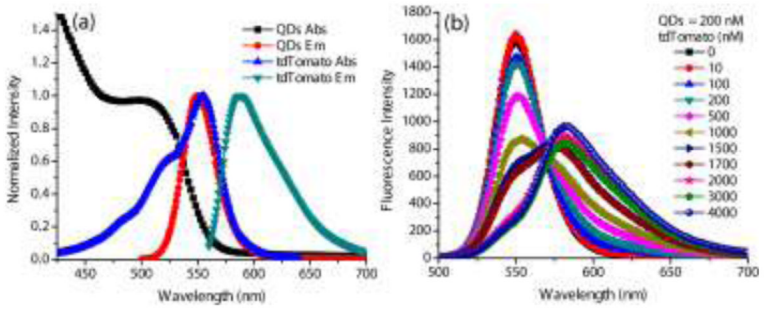

Fig. 2.

(a) Absorption and emission spectra of CdSe/ZnS QDs and tdTomato. (b) Steady-state fluorescence spectra of CdSe/ZnS QDs with increasing concentrations of tdTomato at excitation wavelength 410 nm.

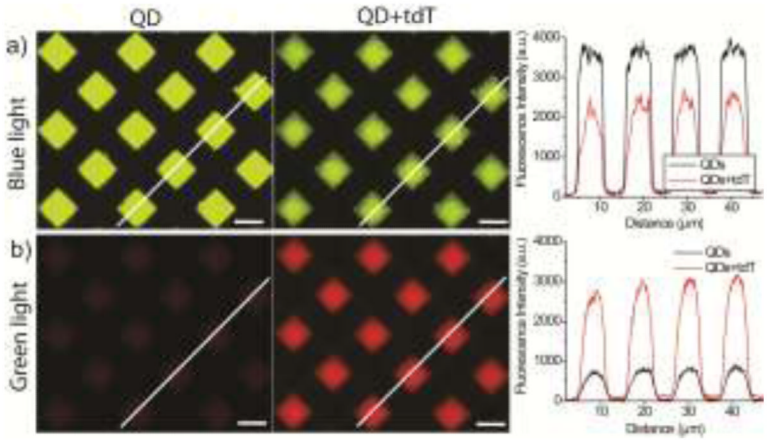

Fig. 3.

Fluorescence images of QD pattern before and after protein immobilization with their intensity map. Scale bars in Fig. 3(a,b) are 5 μm.

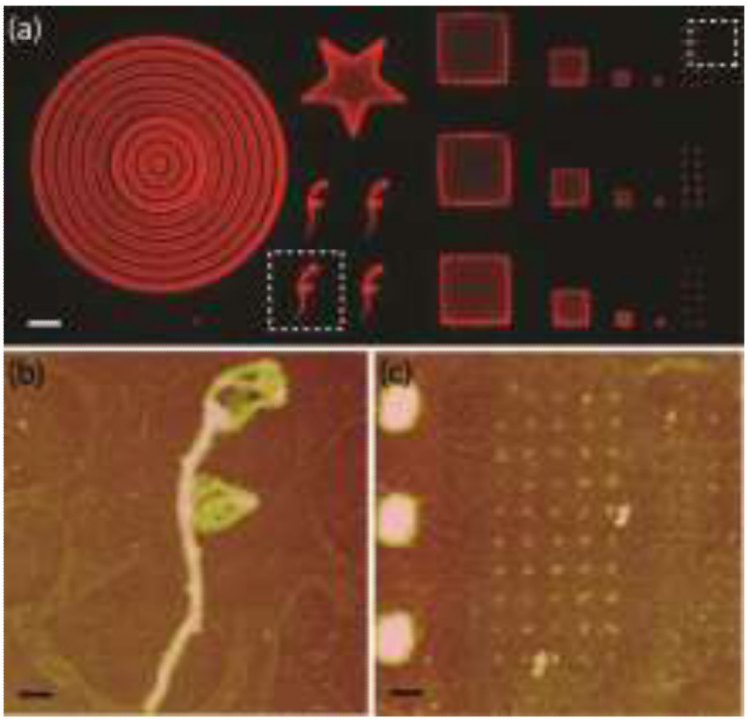

Fig. 4.

(a) Fluorescence image of patterned protein/QD structures of different sizes and shapes. (b) High resolution AFM images of patterned protein/QD nanostructures of (b) a rose and (c) squares of length 500, 100 and 50 nm. Scale bars in Fig. 4(a) and 4(b,c) are 5 μm and 500 nm, respectively.

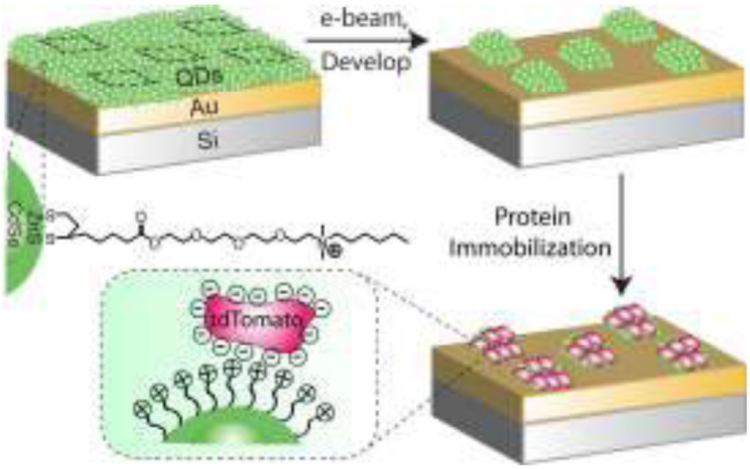

Scheme 1.
Patterning of hybrid protein/QD bionanostructures.